

## Synthesis and Thermal Characterization of Solar Salt-Based Phase Change Composites with Graphene Nanoplatelets

Pethurajan VIGNESHWARAN<sup>1,2</sup>, Saboor SHAIK<sup>1\*</sup>, Sivan SURESH<sup>2</sup>, Müslüm ARICI<sup>3\*</sup>, Asif AFZAL<sup>4</sup>

1. Department of Thermal and Energy Engineering, School of Mechanical Engineering (SMEC), Vellore Institute of Technology, Vellore, Tamil Nadu, India
2. Nanotechnology Research Laboratory, Department of Mechanical Engineering, National Institute of Technology, Tiruchirappalli, Tamil Nadu, India
3. Mechanical Engineering Department, Engineering Faculty, Kocaeli University, Umuttepe Campus, Kocaeli 41001, Turkey
4. Department of Mechanical Engineering, P. A. College of Engineering (affiliated to Visvesvaraya Technological University, Belagavi), Mangaluru 574153, India

© Science Press, Institute of Engineering Thermophysics, CAS and Springer-Verlag GmbH Germany, part of Springer Nature 2023

**Abstract:** Thermal energy storage (TES) systems use solar energy despite its irregular availability and day-night temperature difference. Current work reports the thermal characterizations of solar salt-based phase change composites in the presence of graphene nanoplatelets (GNP). Solar salt (60:40 of NaNO<sub>3</sub>:KNO<sub>3</sub>) possessing phase transition temperature and melting enthalpy of 221.01°C and 134.58 kJ/kg is proposed as a phase change material (PCM) for high-temperature solar-based energy storage applications. Thermal conductivity must be improved to make them suitable for widespread applications and to close the gap between the system needs where they are employed. GNP is added at weight concentrations of 0.1%, 0.3%, and 0.5% with solar salt using the ball milling method to boost its thermal conductivity. Morphological studies indicated the formation of a uniform surface of GNP on solar salt. FTIR spectrum peaks identified the physical interaction between salt and GNP. Thermal characterization of the composites, such as thermal conductivity, DSC and TGA was carried out for the samples earlier and later 300 thermal cycles. 0.5% of GNP has improved the thermal conductivity of salt by 129.67% and after thermal cycling, the enhancement reduced to 125.21% indicating that thermal cycling has a minor impact on thermal conductivity. Phase change temperature decreased by around 2.32% in the presence of 0.5% GNP and the latent heat reduced by 4.34% after thermal cycling. TGA thermograms depicted the composites initiated the weight loss at around 550°C after which it was rapid. After thermal cycling, the weight loss initiated at ~40°C lower compared to pure salt, which was found to be a minor change. Thermal characterization of solar salt and GNP-based solar salt composites revealed that the composites can be used for enhanced heat transfer in high-temperature solar-based heat transfer and energy storage applications.

**Keywords:** thermal energy storage; high temperature; solar salt; graphene nanoplatelets; thermal characterization

Special Column: Recent Advances in PCMs as Thermal Energy Storage in Energy Systems  
Received: Sep 3, 2022

Corresponding author: Saboor SHAIK;  
Müslüm ARICI

GE: MING Tingzhen  
E-mail: saboor.s@vit.ac.in  
muslumarici@gmail.com  
www.springerlink.com

---

**Abbreviations & Symbols**

CF	Copper Foam	PCM	Phase Change Material
CNF	Cellulose Nanofibril	SA	Stearic Acid
CSP	Solar Concentrator Power	SAT	Sodium Acetate Trihydrate
DSC	Differential Scanning Calorimeter	SHS	Sensible Heat Storage
FTIR	Fourier Transform Infrared Spectrometer	$T_{max}$	Maximum temperature in TGA/°C
GNP	Graphene Nanoplatelets	$T_{sc}$	Subcooling temperature/°C
$\Delta H_m$	Latent heat during melting	$T_{wi}$	Initial temperature in TGA/°C
$\Delta H_s$	Latent heat during solidification	TES	Thermal Energy Storage
LFA	Laser Flash Apparatus	TGA	Thermo Gravimetric Analyser
LHS	Latent Heat Storage	X	Zoom

---

## 1. Introduction

Renewable energy sources have received major attention owing to the uneven nature and high price of fossil fuels for power production. Researchers are moving towards renewable-based systems, and since their availability is unpredictable, a feasible energy storage system needs to be designed and integrated with the solar-based system to have an intermittent power supply. Many countries have projected their carbon neutrality and greenhouse gas reduction goals. Utilization of energy storage systems has the main aim of storing energy in a short time and space along with enhancing the energy storage capacity and reducing the emission of hazardous gases and environmental pollution, which further stresses the need to transform from a carbon age to a greener age [1, 2].

### 1.1 Background

Thermal energy storage (TES) method will ameliorate the efficacy of energy utilization and storage. Mostly, thermal energy is stored in the form of sensible or latent heat, depending on the material employed during the energy storage process. Sensible heat storage (SHS) systems are widely employed in industrial sectors where the heat is stored and retrieved based on the temperature rise and drop, respectively. Latent heat storage (LHS) systems work with the phase transition for the storage and release of heat. Comparatively, LHS can be operated with a small temperature difference and has a large energy storage density [3, 4]. LHS systems are mostly employed for solar-based thermal energy storage, and the medium employed to capture the solar energy is phase change materials and possess huge thermal mass and can store more energy compared to SHS systems, and they operate with a small temperature difference during the phase conversion process [5, 6]. Widespread kinds of Phase Change Materials (PCMs) are employed based on melting temperature and their latent heat through the phase conversion process. In addition to the melting point

and latent heat, PCMs should possess high thermal conductivity, which was found to be lower for organic phase change materials. Inorganic PCM have nearly a twofold heat-storage capacity as related to organic PCM. Molten salts come under the category of inorganic PCM, which finds application in two ways such as a sensible heat storage medium as heat transfer fluid in high-temperature solar concentrator power (CSP) systems. Additionally, they are used in LHS medium as PCM, which possesses the additional benefit of high latent heat capacity [7]. The application of molten salts in LHS systems is affected mainly by their thermal conductivity, which lies in the range of 1 W/(m·K) in the solid state and was found to decrease in the liquid state. Except for metal-based materials, all PCMs suffer from the problem of low thermal conductivity, which limits their applications and leads to a low energy storage and release rate, reducing charging and discharging times. Many of the reported works are primarily concerned with overcoming the disadvantage of low thermal conductivity. Many articles have been reported on the incorporation of nanomaterials with PCM, which will reduce the limitations of the PCM and allow it to be utilized for a wider range of applications that require enhanced thermal performance [8].

### 1.2 Literature review

Many studies have reported on the different ways to upsurge the thermal properties of the PCM. Blending the PCM with various concentrations of nanoparticles has given added advantages such as increasing the thermal conductivity, regulating the phase segregation, and neglecting incongruent melting. Cupric oxide (CuO) was added with nitrate salts of potassium nitrate, sodium nitrate, and their eutectics [9] and were found to melt at 334°C, 306°C, and 222°C, respectively and reported that the addition of 2% CuO improved thermal conductivity to a temperature of 150°C while maintaining high chemical stability. Li et al. [10] blended stearic acid (SA) with copper foam (CF) to prepare composite PCMs via

molten impregnation method and reported that liquid SA and SA/CF (40 PPI) have improved internal heat transfer consistency. Zirui et al. [11] dispersed graphene nanoplatelets (GNP) into 1-tetradecanol with loadings up to 3 wt% and reported that heat storage and heat transfer rates during melting slow down to some extent for all geometrical and thermal configurations in a differentially heated rectangular cavity. A eutectic triple carbonate salt ( $\text{Li}_2\text{CO}_3\text{-Na}_2\text{CO}_3\text{-K}_2\text{CO}_3$ ) was used as an energy storage medium in CSP plants [12] where magnesium (Mg) particles were blended with the PCM and was found to have latent heat of 160 J/g and thermal conductivity of 1.93 W/(m·K) with Mg loading of 2%. Recently, cellulose nanofibril (CNF) was used as a biopolymer to support the distribution of silver nanoparticles with sodium acetate trihydrate (SAT) [13] and thermal conductivity enhanced by 31.6% as compared to SAT with an enthalpy decrease of 2% after 100 thermal cycles. Copper nanoparticles were dispersed in solar salt by Saranprabhu et al. [14] with a varied concentration of 0–0.5 weight percent for application in solar TES for industrial application and reported a thermal conductivity enhancement of 11% with the concentration of 0.5% at 180°C along with an increase in the discharge capacity of 42.4% and the formed composites retained their thermal properties after 1000 thermal cycles. Another study reported by Zhang et al. [15] worked on the incorporation of ceramic foam with solar salt for medium-temperature TES and reported that the melting rate enhancement of 41.3% along with an enhancement of energy storage rate of 40.3% as related to pure solar salt.

Solar salt (60:40 of  $\text{NaNO}_3\text{:KNO}_3$ ) with a transition temperature in the range of 222°C–225°C is a common heat transfer fluid and a heat storage medium in high-temperature solar-based heat transfer and energy storage applications owing to its great thermal solidity [16, 17]. Saranprabhu and Rajan [18] prepared composites of solar salt by dispersing different concentrations of Magnesium oxide (MgO) nanoparticles to study their effect on the thermal properties of PCM and found that thermal conductivity escalated by 17.5% after the addition of 0.5% of MgO along with a decrease in solidification time by 30%. Anagnostopoulos et al. [19] studied the wetting and rheological behaviour after the addition of  $\text{SiO}_2$  nanoparticles with solar salt and reported that viscosity increased when 1% of silica is added to PCM. Muñoz-Sánchez et al. [20] reported on the viscosity of eight solar salt-based nanofluids comprising silica and alumina nanoparticles using rheometers and varying shear rates and temperatures, where viscosity was measured through the coaxial cylinder method. Mao et al. [21] reported on the dynamic simulation along with experimental techniques to determine the variations in the freezing point,

supercooling, and enthalpy of solidification of solar salt in the presence of  $\text{Al}_2\text{O}_3$  and  $\text{SiO}_2$  and found that  $\text{Al}_2\text{O}_3$  and  $\text{SiO}_2$  promote heterogeneous nucleation along with a reduction in supercooling, and concluded that  $\text{Al}_2\text{O}_3$  has a more significant effect on nucleation.

### 1.3 Novelty of the work

Significant research has been reported on the usage of solar salt as a direct heat transfer fluid in high-temperature heat transfer applications, with less research on using them as a heat storage medium in TES applications. We worked on the encapsulation of solar salt [22] and the addition of  $\text{Al}_2\text{O}_3$  and  $\text{TiO}_2$  nanoparticles to solar salt [23] and proposed them for heat storage applications.

(1) The current study is a comprehensive work that included thermal and physical characterization studies on solar salt with varying weight percents of graphene nanoplatelets, along with thermal cycling studies to confirm their thermal stability after repeated cycles.

(2) To boost their heat transfer rate and also to reduce the time taken for charging the PCM in the presence of heat, we have added GNP as a thermal conductivity enhancer, which marks the primary novelty of the current work.

(3) Additionally, thermal cycling studies are done to ensure that the thermal and physical properties have not altered after the addition of GNP and also due to repeated charging and discharging processes, which marks the second novelty of the current work.

Based on these, the samples of nano enhanced solar salt were prepared with a varied concentration of GNP, and thermal cycling was done for 300 cycles followed by their thermophysical characterization, which is also reported in the current work.

## 2. Experimental Methodology

### 2.1 Selection of materials

The present study involves the utilization of an eutectic mixture comprising Sodium nitrate ( $\text{NaNO}_3$ ) and Potassium nitrate ( $\text{KNO}_3$ ) in a precise weight ratio of 60:40. This well-known compound is commonly referred to as solar salt and serves as the phase change material. The precursor substances were acquired from Spectrum Chemicals, India. As an enhancer of thermal conductivity, graphene nanoplatelets were chosen and sourced from Sigma Aldrich. These materials were employed in their original state without undergoing any supplementary purification processes.

### 2.2 Preparation of eutectic mixture

The process of low energy ball milling was employed to create the eutectic mixture of nitrate salts. To initiate

this process, the sample holder was filled with the precise amount of the salts, following which three steel balls were carefully placed inside the container alongside the sample. Through the application of the centrifugal force principle, the sample holder was set into rotation. The rotational speed was maintained at a constant 300 r/min for a duration of 200 minutes. This specific combination of speed and time resulted in the formation of a homogeneous blend of solar salt.

### 2.3 Preparation of GNP enhanced solar salt

The solar salt, as detailed in Section 2.2, will serve as the foundation for subsequent preparations. The process of low energy ball milling is then employed to create nano-enhanced solar salt. Nanoparticles are carefully measured according to their concentration and introduced into the sample holder containing the solar salt. Subsequently, the sample holder undergoes rotation for an additional 150 minutes at a consistent speed of 300 r/min. This duration and speed combination facilitates the production of nano-enhanced solar salt. This exact procedure is iterated to prepare the remaining nano-enhanced PCM composites.

### 2.4 Thermal cycling of GNP enhanced solar salt

The technique employed to assess the thermal reliability of the samples is referred to as thermal cycling. This approach involves subjecting the sample to a temperature cycle that starts at room temperature and reaches a temperature exceeding the sample's melting point, followed by cooling back to room temperature. This

constitutes a single thermal cycle. As per findings from our previously published article [22] concerning solar salt, there was a minor decline in properties following thermal cycling. This can be attributed to factors such as alterations in chemical composition, weight loss of the sample, or the presence of impurities. Within our laboratory, we designed an open thermal cyclers for this purpose. It comprises a flat plate heater with a power capacity of 1000 W, capable of reaching temperatures of up to 500°C. The heater is equipped with a K-type thermocouple for precise temperature measurement. To conduct the thermal cycling, the sample is positioned in a glass crucible and covered with aluminum foil. The temperature is then set to 230°C to initiate sample melting. This entire process is repeated for a total of 300 cycles. For visual reference, Fig. 1 provides an illustration of the thermal cyclers utilized in this study.

## 3. Characterisation of GNP-Enhanced Solar Salt

Thermal and physical characterization of pure and GNP enhanced solar salt has been studied to know about the impact of GNP with solar salt. Morphological studies were carried out using VEGA 3 TESCAN Scanning Electron Microscope which has an intensification of 2.5 to 1 000 000 X alongside accelerating voltage of 200 to 30 kV. LFA 467 Laser flash apparatus was used to measure thermal conductivity which works in temperature range from -100°C to 500°C and can measure thermal diffusivity from 0.001–2000 mm<sup>2</sup>/s and thermal conductivity from 0.1–4000 W/(m·K) in a nitrogen atmosphere. The presence of functional groups was identified using Perkin Elmer Spectrum 2 Infrared Spectrophotometer in the wavenumber range of 500–4000 cm<sup>-1</sup>. Phase change properties were studied using DSC 6000 Perkin Elmer which works in temperature range of -180°C to 450°C, heating and cooling rates can be varied in the range of 0.1°C/min to 100°C/min and analysis is carried out in nitrogen atmosphere. TGA 4000 Perkin Elmer was utilized to study about the thermal deterioration of the composites in a nitrogen environment and the instrument works in temperature range: 30°C to 1000°C, heating rate can be varied from 0.1°C/min and 200°C/min

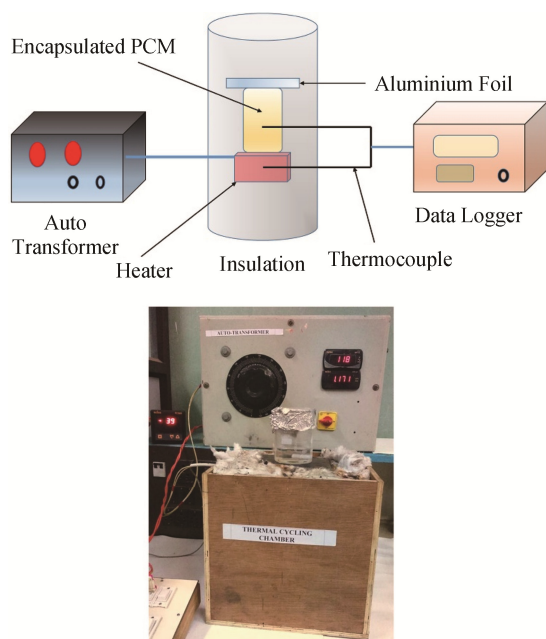


Fig. 1 Thermal cyclers used in the current study

## 4. Results and Discussion

### 4.1 Morphological study of the composites

The morphology of synthesized composites was studied using a Scanning Electron Microscope (SEM) (VEGA 3 TESCAN) (Fig. 2). At room temperature, solar salt is white, and after the addition of GNP, the colour of the composites changed to a dark complexion due to the presence of GNP. Fig. 2(a) depicts the SEM image of the

solar salt, where we can visualise the crystal structure size is not uniform. Fig. 2(b) depicts the SEM image of solar salt after the addition of 0.1% (weight) of GNP. We can visualize the GNP getting adhered to the surface of the solar salt, and the GNP did not agglomerate with the solar salt and it was found to be evenly distributed.

#### 4.2 Thermal conductivity of phase change composites

The thermal conductivity of a PCM plays a key role in determining the efficiency of the TES system and also has an impact on the design of the system. In the current work, the thermal conductivity of the samples was calculated at an ambient condition in a nitrogen atmosphere using the Laser Flash Apparatus (LFA 457). The addition of high-conducting nanomaterial to the irregularly shaped PCM will lead to the development of a thermal network that enhances the thermal conductivity of the PCM. The sample preparation and the procedure to calculate the thermal conductivity are the same as those reported in our previous work [22, 23]. Table 1 lists the thermal conductivity of the nano-enhanced PCM with regard to thermal cycling.

In our current study on nano-enhanced solar salt, we have added graphene nanoplatelets to increase the thermal conductivity, and we observed a linear upsurge in thermal conductivity with an upsurge in the concentration of GNP. Pure solar salt was found to have a thermal conductivity of 0.809 W/(m·K), and increased to 1.058 W/(m·K), 1.453 W/(m·K), and 1.858 W/(m·K) after the addition of 0.1%, 0.3%, and 0.5% (weight) of GNP with solar salt. Thermal conductivity was found to escalate by 30.77%, 79.60%, and 129.67% after the addition of

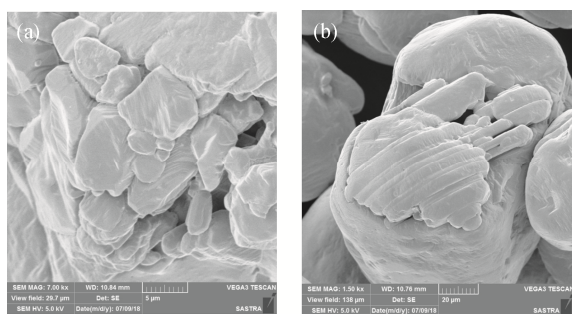


**Fig. 2** SEM images of pure and nano-enhanced solar salt

0.1%, 0.3%, and 0.5% of GNP respectively. It was found that the addition of GNP has formed an internal network that holds the PCM, forming a continuous heat conduction network that transmits the phonons, thereby increasing the thermal conductivity [24].

Thermal cycling of the samples led to a minor reduction in thermal conductivity which was found to be minimal in terms of the efficiency of the TES system. Pure salt was found to have a thermal conductivity of 0.809 W/(m·K), and after thermal cycling, it reduced to 0.780 W/(m·K). The reduction in thermal conductivity was significant, and it is mainly due to the repeated thermal cycles. After the addition of GNP, the same trend was witnessed. 1.058 W/(m·K), 1.453 W/(m·K), and 1.858 W/(m·K) were the thermal conductivities after the addition of 0.1%, 0.3%, and 0.5% of GNP and the same were reduced to 1.041 W/(m·K), 1.439 W/(m·K), and 1.822 W/(m·K), respectively. From the thermal cycling process, we can infer that the nanoparticles and PCM have not lost their thermal properties even after 300 thermal cycles.

#### 4.3 Chemical compatibility of the composites

FT-IR spectrum peaks were used to investigate the chemical configuration of phase change composites. A predictable KBr disc method was used to illustrate the FTIR spectra in frequency regions ranging from 400  $\text{cm}^{-1}$  to 4000  $\text{cm}^{-1}$ . Figs. 3(a) and 3(b) depict the FTIR spectrum peaks of the samples' earlier and later thermal cycling respectively. It can be seen that all the curves are relatively alike in the spectrum region. The distinctive peaks at 2436.75  $\text{cm}^{-1}$  and 1389.03  $\text{cm}^{-1}$  designate the existence of nitrate in  $\text{KNO}_3$ . For all composites, a peak originated at 3471.22  $\text{cm}^{-1}$  which is attributed to the hydroxyl (O-H) stretch and additional bend of  $\delta$ -OH at 1789.21  $\text{cm}^{-1}$  and 1741.28  $\text{cm}^{-1}$  signifying the vanishing of water from the sample. A wide peak at 1389.25  $\text{cm}^{-1}$  specifies the  $\nu_3 \text{NO}_3^-$  stretch. The peak at 851.89  $\text{cm}^{-1}$  is sturdy and demonstrates the existence of sodium nitrate crystals. From the FTIR spectrum of composites after cycling, it is obvious that frequency persisted relatively alike throughout. The outcomes reveal that only physical contact took place between GNP and salt in the absence of any chemical reaction.

**Table 1** Thermal conductivity of pure and nano-enhanced phase change materials

Phase change material	Thermal conductivity/W·(m·K) <sup>-1</sup>		Enhancement/%	
	Before thermal cycling	After thermal cycling	Before thermal cycling	After thermal cycling
Pure Salt	0.809	0.780	–	–
Salt+0.1% GNP	1.058	1.041	30.77	28.67
Salt+0.3% GNP	1.453	1.439	79.60	77.87
Salt+0.5% GNP	1.858	1.822	129.67	125.21

#### 4.4 Phase transition properties of phase change composites

Differential scanning calorimetric investigation was used to find the phase conversion properties of the PCM. The samples were heated initially beyond their phase change temperature and later chilled to room temperature to maintain uniformity. The second and third cycle values were noted, and the average of the three cycles was taken as the final results of the corresponding sample. DSC estimates the quantity of heat captivated or released concerning the reference sample. The latent heat during melting and solidifying is calculated by the integration of the area underneath the peaks by sketching a tangential line from the peak onset to its corresponding offset.

The DSC thermograms of pure salt and nano-enhanced salt showed two peaks. A minor peak in the temperature range of 110°C–120°C is the solid-solid transition, and the main peak in the temperature range of 215°C–225°C represents the solid-liquid phase change from which the phase change temperatures along with their corresponding latent heats are determined. Table 2 lists the phase change properties of PCM before thermal cycling.

Fig. 4(a) depicts the DSC thermograms of pure and nano-enhanced solar salt before thermal cycling. Pure salt was seen to thaw and freeze at 221.01°C and 214.63°C. Latent heat was found to be 134.58 kJ/kg and 108.91 kJ/kg for the melting and solidification processes, respectively. The addition of GNP reduced the latent heat

with only a minor change in phase transition temperatures. With the addition of 0.1% GNP, the melting and solidification happened at 221.48°C and 214.16°C, respectively, with the corresponding enthalpies being 130.81 kJ/kg and 103.42 kJ/kg. The properties changed further when the nanoparticle concentration was increased. At 0.3% and 0.5%, the melting points measured were 214.16°C and 215.48°C, respectively. The reduction in melting point was found to be 6.85°C and 5.58°C correspondingly, as related to pure salt. When compared to pure salt, latent heat was found to be significantly reduced. Latent heat was found to be 123.85 and 118.95 kJ/kg during melting and 98.62 kJ/kg and 92.56 kJ/kg during solidification, respectively, for 0.3% and 0.5% concentrations of GNP. This is because the nanomaterials have acted as nucleating agents for the PCM and altered their thermal properties, and also because more energy is utilized to break the molecular bonds during the heat charging process [25].

Fig. 4(b) depicts the DSC thermograms of pure and nano-enhanced solar salt after thermal cycling, and Table 3 lists the phase conversion properties of PCM after thermal cycling. It is quite obvious that thermal cycling has a minor effect on the thermal properties of the PCM. Following that, pure salt was discovered to thaw and freeze at 219.91°C and 211.03°C, respectively, with corresponding latent heats of 132.86 kJ/kg and 105.56 kJ/kg. The change in the latent heat was found to be

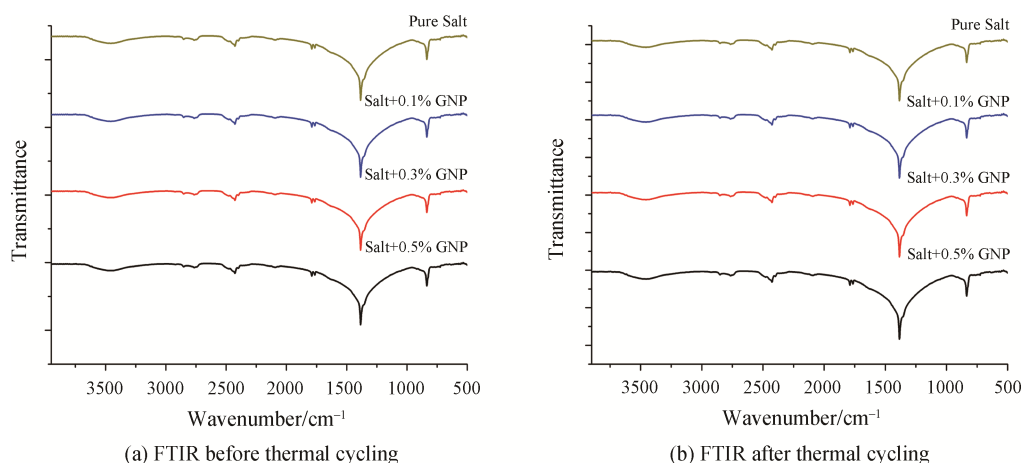


Fig. 3 FTIR spectrum peaks pure and nano-enhanced phase change materials

Table 2 Phase change properties before thermal cycling

Phase change material	Melting		Solidification		Subcooling
	$T_m/^\circ\text{C}$	$\Delta H_m/\text{kJ}\cdot\text{kg}^{-1}$	$T_s/^\circ\text{C}$	$\Delta H_s/\text{kJ}\cdot\text{kg}^{-1}$	$T_{sc}/^\circ\text{C}$
Pure Salt	221.01	134.58	214.63	108.91	6.38
Salt+0.1% GNP	221.48	130.81	214.16	103.42	7.32
Salt+0.3% GNP	214.16	123.85	207.86	98.62	6.30
Salt+0.5% GNP	215.48	118.95	206.60	92.56	8.88

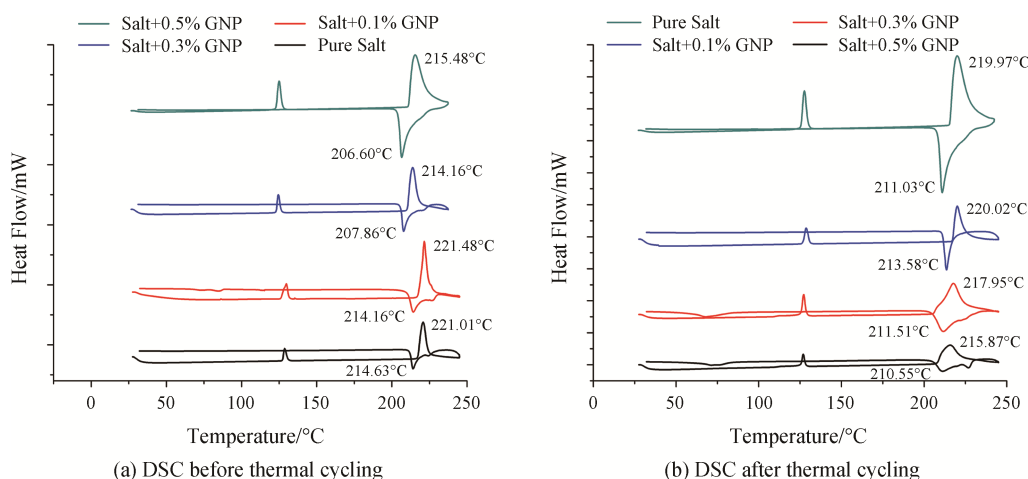


Fig. 4 DSC thermograms of pure and nano-enhanced PCMs

Table 3 Phase change properties after thermal cycling

Phase change material	Melting		Solidification		Subcooling $T_{sc}/^{\circ}\text{C}$
	$T_m/^{\circ}\text{C}$	$\Delta H_m/\text{kJ}\cdot\text{kg}^{-1}$	$T_s/^{\circ}\text{C}$	$\Delta H_s/\text{kJ}\cdot\text{kg}^{-1}$	
Pure Salt	219.97	132.86	211.03	105.56	8.94
Salt+0.1% GNP	220.02	127.52	213.58	98.87	6.44
Salt+0.3% GNP	217.95	119.75	211.51	91.92	6.44
Salt+0.5% GNP	215.87	114.82	210.55	85.72	5.32

Table 4 Percentage change in thermal properties after thermal cycling

Phase change material	Melting/%		Solidification/%	
	$T_m$	$\Delta H_m$	$T_s$	$\Delta H_s$
Pure Salt	0.47	1.27	1.67	3.07
Salt+0.1% GNP	0.44	5.24	0.48	9.21
Salt+0.3% GNP	1.38	11.01	1.45	15.60
Salt+0.5% GNP	2.32	13.20	1.90	21.29

1.27% and 3.07%, respectively, during melting and solidifying, compared to pure salt. The percentage change in the nano-enhanced PCM as compared to the pure salt is listed in Table 4. Following that, a negligible decrease in latent heat was discovered, and the trend continues as their concentration increases. The enthalpy reduction was found to be greater throughout the solidification process as compared to the melting process. The lessening in the latent heat is because GNP has not taken part in the melting and solidification processes [26].

#### 4.5 Subcooling degree

The sub-cooling temperature of a PCM plays a major part in the determination of the crystallization process. It is the variance in melting and solidification temperatures. Subcooling will be high in the case of organic PCM. In our work, the pure solar salt had a subcooling

temperature of 6.38°C, which was found to be minimal in its application in high-temperature heat storage systems. After the addition of GNP, the subcooling temperature was found to be 7.32°C, 6.30°C, and 8.88°C for 0.1%, 0.3%, and 0.5%, respectively, before thermal cycling. The sub-cooling degree after thermal cycling showed a minor change due to the alteration in the melting and solidification temperatures of PCM. After thermal cycling, pure salt had a subcooling of 8.94°C. After the addition of GNP, this value was found to be 6.44°C, 6.44°C and 5.32°C with 0.1%, 0.3%, and 0.5% respectively.

#### 4.6 Thermal steadiness of phase change composites

The thermal steadiness of PCMs must be high for their application in the TES system. Thermogravimetric analysis is the technique that is predominantly used to examine the thermal consistency of the PCM. In TGA, stability is checked for an increase in temperature, which in turn gives the change in weight with respect to temperature. Fig. 5(a) denotes the TGA data of pure and nano-enhanced salt before thermal cycling. All the samples were found to have a single and gradual weight loss with respect to temperature. The decomposition temperature is determined by the intersection of the tangents in horizontal and vertical segments where the curve starts to have a rapid weight loss. The weight loss

was found to be minimal until the temperature of 550°C after which the weight loss was initiated. This denotes that the salt and nano-enhanced salt can endure a temperature of nearly 550°C without any weight loss and can be used as a loading medium in high-temperature TES systems. Pure salt started to lose its weight at a temperature of 575.68°C and was rapid until 683.75°C. The weight loss temperature decreased to 57.46°C with 0.1% of GNP. When the concentration was increased, the weight loss temperature was found to be 544.23°C and 561.37°C after 0.3% and 0.5% of GNP respectively. The weight loss was rapid till 685.06°C, 682.41°C, and 680.47°C after 0.1%, 0.3%, and 0.5% of GNP, respectively.

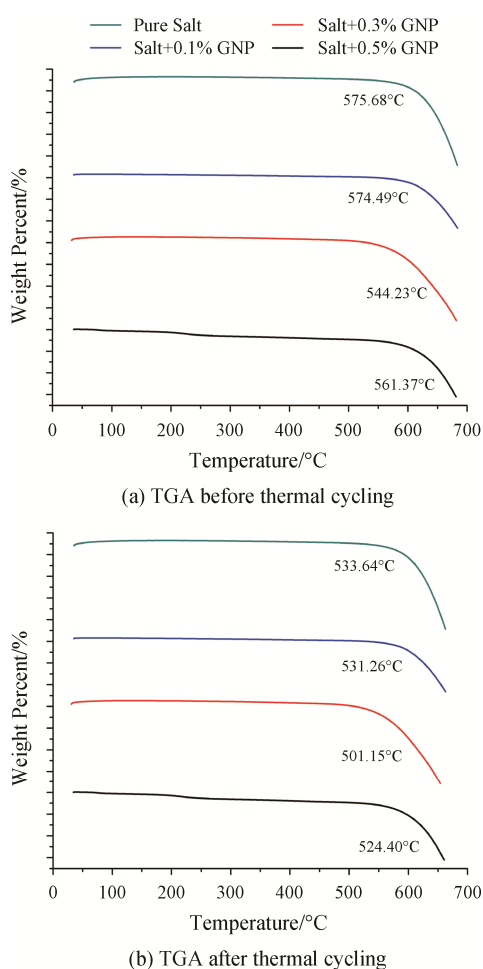


**Fig. 5** TGA Thermograms of pure and nano-enhanced PCMs

The summary of TGA data is listed in Table 5. From the TGA analysis of the samples' earlier and later thermal cycling, we can infer that pure salt and nano-enhanced salt have the requirements for high-temperature TES systems. Fig. 5(b) depicts the TGA thermograms of the samples after thermal cycling. Thermal cycling did not have a major influence on the thermal stability of the samples. A temperature difference of around 20°C was

found where the weight loss initiated. After thermal cycling, the weight loss commenced at around 530°C, and before thermal cycling, it was found to be 550°C. The weight loss was initiated at 533.64°C for pure salt after thermal cycling, and it was rapid until 664.37°C. In the presence of GNP, weight loss started at 531.26°C, 501.15°C, and 524.40°C and was rapid till 663.18°C, 653.34°C, and 662.14°C for 0.1%, 0.3%, and 0.5% of GNP, respectively.

**Table 5** Summary of TGA data

Phase change material	Before thermal cycling		After thermal cycling	
	$T_{wi}/^{\circ}\text{C}$	$T_{max}/^{\circ}\text{C}$	$T_{wi}/^{\circ}\text{C}$	$T_{max}/^{\circ}\text{C}$
Pure Salt	575.68	683.75	533.64	664.37
Salt+0.1% GNP	574.49	685.06	531.26	663.18
Salt+0.3% GNP	544.23	682.41	501.15	653.94
Salt+0.5% GNP	561.37	680.47	524.40	662.14

The TGA analysis of the salts with nanomaterials showed a significant variation in thermal properties after thermal cycling. The weight deprivation was found to be less for pure salt when equated to the salt after thermal cycling. The weight loss due to thermal cycling may be due to the presence of impurities, chemical reactions, or decomposition of the PCM. DSC studies indicated that there was no change in chemical reactions where the thermal properties remained unaltered. So, weight deprivation is typically due to the decomposition and disappearance of the salt at higher temperatures. We can conclude that salt and salt composites were thermally stable for temperatures up to 550°C after which we could experience rapid weight loss. Moreover, the composites were found to maintain their stability after thermal cycles.

## 5. Conclusions and Future Recommendations

Solar salt has been extensively used as a heat transfer fluid and energy storage medium for solar-based heat transfer and TES applications. The current study reports the thermal and physical characterization studies on solar salt with varying weight percents of graphene nanoplatelets, along with an insight on the thermal cycling studies to confirm their thermal stability after repeated cycles. The major observations are listed below.

(1) Morphological studies indicated the formation of a cluster of GNP on the surface of solar salt. FTIR spectrum peaks depicted the presence of physical interaction with an absence of chemical interaction between PCM and GNP.

(2) Thermal conductivity was found to be 0.809 W/(m·K) and 0.780 W/(m·K) previously and afterwards thermal cycling. PCM composites were found to have

enhanced thermal conductivities of 1.058 W/(m·K), 1.453 W/(m·K), and 1.858 W/(m·K) after the addition of 0.1%, 0.3%, and 0.5% of GNP before thermal cycling. After thermal cycling, thermal conductivities were found to be 1.041 W/(m·K), 1.439 W/(m·K), and 1.822 W/(m·K) in the presence of 0.1%, 0.3%, and 0.5% of GNP.

(3) Pure salt was found to thaw and freeze at 221.01°C and 214.63°C, respectively. After thermal cycling, these values were 219.97°C and 211.03°C, respectively. In the presence of 0.5% GNP, the melting and solidification points followed a decreasing trend of 2.32%.

(4) The melting latent heat of pure salt (134.58 kJ/kg) reduced to 132.86 kJ/kg after thermal cycling. After the addition of 0.5% GNP, the enthalpy was found to be 118.95 kJ/kg and 114.82 kJ/kg earlier and later thermal cycling, respectively.

(5) TGA analysis showed the salt and composites were thermally stable till 550°C, after which the weight loss was initiated. Pure salt initiated weight loss at 575.68°C with a rapid weight loss until 683.75°C. After thermal cycling, it was measured to be 533.64°C and 664.37°C for initiation and rapid weight loss, respectively.

The thermal analysis of both solar salt and the composites incorporating GNP (graphene nanoplatelets) has highlighted their potential for improving heat transfer in solar-based high-temperature heat transfer and thermal energy storage (TES) systems. The main challenge with these salts lies in their inherently low conductivity, which has been partially mitigated through the incorporation of nanomaterials. This, in turn, has sparked additional research into reducing latent heat. Looking ahead, there is scope for further exploration. This could involve introducing a broader variety of nanomaterials into solar salt, alongside an investigation into the underlying mechanisms behind the reduction of latent heat in the presence of these nanomaterials. Such endeavours would contribute to advancing the field and expanding the knowledge surrounding enhanced heat transfer and thermal energy storage systems.

### Conflict of Interest

On behalf of all authors, the corresponding author states that there is no conflict of interest.

### References

- [1] Lu H., Zhang X., Ji J., et al., Research progress on the influence of nano-additives on phase change materials. *Journal of Energy Storage*, 2022, 55: 105807.
- [2] Prakhar D., Reddy V.J., Parvate S., et al., Salt hydrate phase change materials: Current state of art and the road ahead. *Journal of Energy Storage*, 2022, 51: 104360.
- [3] Atul S., Tyagi VV., Chen CR., et al., Review on thermal energy storage with phase change materials and applications. *Renewable and Sustainable Energy Reviews*, 2009, 13(2): 318–345.
- [4] Hasnain S.M., Review on sustainable thermal energy storage technologies, Part I: heat storage materials and techniques. *Energy Conversion and Management*, 1998, 39(11): 1127–1138.
- [5] Jegadheeswaran S., Pohekar S.D., Performance enhancement in latent heat thermal storage system: a review. *Renewable and Sustainable Energy Reviews*, 2009, 13(9): 2225–2244.
- [6] Francis A., Hewitt N., Eames P., Smyth M., A review of materials, heat transfer and phase change problem formulation for latent heat thermal energy storage systems (LHTESS). *Renewable and Sustainable Energy Reviews*, 2010, 14(2): 615–628.
- [7] Kenisarin M.M., High-temperature phase change materials for thermal energy storage. *Renewable and Sustainable Energy Reviews*, 2010, 14(3): 955–970.
- [8] Changlu X., Zhang H., Fang G., Review on thermal conductivity improvement of phase change materials with enhanced additives for thermal energy storage. *Journal of Energy Storage*, 2022, 51: 104568.
- [9] Jr M., Philip D., Alam T.E., et al., Nitrate salts doped with CuO nanoparticles for thermal energy storage with improved heat transfer. *Applied Energy*, 2016, 165: 225–233.
- [10] Chuanchang L., Zhao X., Zhang B., et al., Stearic acid/copper foam as composite phase change materials for thermal energy storage. *Journal of Thermal Science*, 2020, 29(2): 492–502.
- [11] Zirui L., Hu N., Tu J., et al., Experimental investigation of heat storage and heat transfer rates during melting of nano-enhanced phase change materials (NEPCM) in a differentially-heated rectangular cavity. *Journal of Thermal Science*, 2020, 29(2): 503–511.
- [12] Heqing T., Du L., Wei X., et al., Enhanced thermal conductivity of ternary carbonate salt phase change material with Mg particles for solar thermal energy storage. *Applied Energy*, 2017, 204: 525–530.
- [13] Zhenghui S., Oh K., Kwon S., et al., Use of cellulose nanofibril (CNF)/silver nanoparticles (AgNPs) composite in salt hydrate phase change material for efficient thermal energy storage. *International Journal of Biological Macromolecules*, 2021, 174: 402–412.
- [14] Saranprabhu M.K., Rajan K.S., Copper-dispersed solar salt: An improved phase change material for thermal energy storage. *Thermochimica Acta*, 2022, 716: 179302.
- [15] Shuai Z., Yao Y., Jin Y., et al., Heat transfer characteristics of ceramic foam/molten salt composite phase change material (CPCM) for medium-temperature thermal energy storage. *International Journal of Heat and*

- Mass Transfer, 2022, 196: 123262.
- [16] Yuhang Z., Zhang M., Cheng F., et al., Experimental investigation of the migration and solidification characteristics of solar salt in hot sand layer of tank foundation. *Applied Thermal Engineering*, 2023, 219: 119571.
- [17] Ming L., Saman W., Bruno F., Review on storage materials and thermal performance enhancement techniques for high temperature phase change thermal storage systems. *Renewable and Sustainable Energy Reviews*, 2012, 16(4): 2118–2132.
- [18] Saranprabhu M.K., Rajan K.S., Magnesium oxide nanoparticles dispersed solar salt with improved solid phase thermal conductivity and specific heat for latent heat thermal energy storage. *Renewable Energy*, 2019, 141: 451–459.
- [19] Argyrios A., Palacios A., Navarro M.H., et al., Effect of SiO<sub>2</sub> nanoparticle addition on the wetting and rheological properties of solar salt. *Solar Energy Materials and Solar Cells*, 2020, 210: 110483.
- [20] Sánchez B.M., Maestre J.N., Veca E., et al., Rheology of Solar-Salt based nanofluids for concentrated solar power. Influence of the salt purity, nanoparticle concentration, temperature and rheometer geometry. *Solar Energy Materials and Solar Cells*, 2018, 176: 357–373.
- [21] Rui M., Yang Q., Li Z., et al., Analysis of scale and frame interface effects on the solidification properties of solar salt in mesopores. *Solar Energy Materials and Solar Cells*, 2022, 247: 111949.
- [22] Vignesh P., Suresh S., Mojiri A., et al., Microencapsulation of nitrate salt for solar thermal energy storage-synthesis, characterisation and heat transfer study. *Solar Energy Materials and Solar Cells*, 2020, 206: 110308.
- [23] Jeyaseelan T.R., Azhagesan N., Pethurajan V., Thermal characterization of NaNO<sub>3</sub>/KNO<sub>3</sub> with different concentrations of Al<sub>2</sub>O<sub>3</sub> and TiO<sub>2</sub> nanoparticles. *Journal of Thermal Analysis and Calorimetry*, 2019, 136(1): 235–242.
- [24] Xi S., Wang Z., Wu Y., et al., Effect of functionalization on thermal conductivities of graphene/epoxy composites. *Carbon*, 2016, 108: 412–422.
- [25] Shahin S., Kargarsharifabad H., Mirjalily S.A.A., A comprehensive review of nano-enhanced phase change materials on solar energy applications. *Journal of Energy Storage*, 2022, 50: 104262.
- [26] D'Oliveira E.J., Pereira S.C.C., Groulx D., et al., Thermophysical properties of Nano-enhanced phase change materials for domestic heating applications. *Journal of Energy Storage*, 2022, 46: 103794.